ISBN: 978-3-95450-234-9 ISSN: 2673-5504 doi:10.18429/JACoW-SRF2023-TUPTB014

DEVELOPMENT OF Nb_3Sn COATING SYSTEM AND RF MEASUREMENT RESULTS AT KEK

H. Ito[1,*], H. Sakai[1], K. Umemori[1], T. Yamada[1], KEK, Tsukuba, Ibaraki, Japan
K. Takahashi, SOKENDAI, Tsukuba, Ibaraki, Japan
[1] also at SOKENDAI, Tsukuba, Ibaraki, Japan

Abstract

We have constructed an Nb_3Sn cavity coating system based on the Sn vapor diffusion method. After the construction, our coating system and environment have been improved through sample and cavity coating tests. Our cavity achieves a Q_0 above 1×10^{10} at 4 K after improvement. We will report on the detail of improvement on our coating system and RF measurement results of single-cell Nb_3Sn cavities.

INTRODUCTION

Nb_3Sn is one of the leading candidates for SRF cavity materials because it has the potential to operate cavities at higher temperatures with a higher Q_0 and achieve a higher accelerating gradient [1]. Focusing on the operating temperature, since the transition temperature of Nb_3Sn is twice that of Nb, Nb_3Sn cavities can achieve Q_0 comparable to conventional Nb cavities at 4.2 K. In other words, the Nb_3Sn cavity has an attractive future potential to operate without liquid helium and with conduction cooling by cryocoolers and research for this purpose is actively underway [2–6]. Development of Nb_3Sn cavities has been actively carried out using a variety of methods [1], among which the thermal diffusion method is more advanced than others in terms of practical application [7–12]. We also started the development of Nb_3Sn cavities based on the thermal diffusion method in 2019 [13, 14]. Through furnace heating tests and sample Nb_3Sn coating tests, we have understood the characteristics of our furnace and have performed Nb_3Sn coating on single-cell cavities a total of four times so far.

FIRST Nb_3Sn COATING ON SINGLE-CELL CAVITY

After establishing the capability to form Nb_3Sn films on Nb substrates through sample coating tests, the first Nb_3Sn coating test was performed on a 1.3 GHz single-cell cavity, as shown in Fig. 1. The coating furnace has two heating systems, one that heats the entire furnace and one that heats the Sn crucible independently. During coating, the Sn crucible is heated to a higher temperature than the furnace to actively evaporate Sn. The surface of the cavity after the coating is visually darker gray than niobium and matte.

Figure 2 shows the $Q - E$ curves measured at 4.2 K for the single-cell cavity before and after the first coating. The first-coated cavity shows a Q_0 of 3.9×10^9 at 4.2 K and at low field which is 5 times higher than that of the Nb cavity.

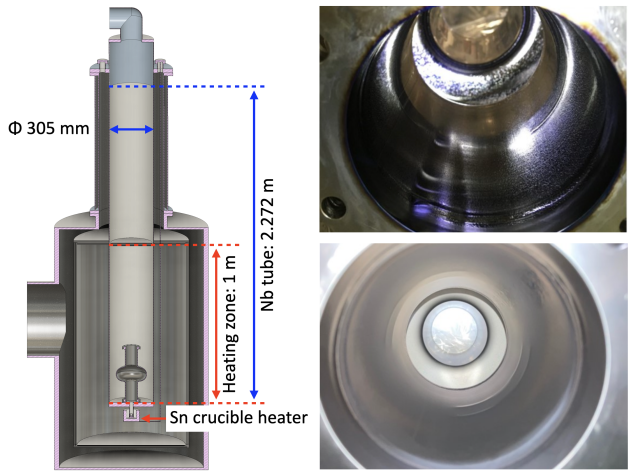

Figure 1: Cross-section of coating furnace (left), inside of cavity before (top right), and after first coating (bottom right).

However, this Q_0 is lower than the expected value of 1×10^{10} and shows a significant Q-slope.

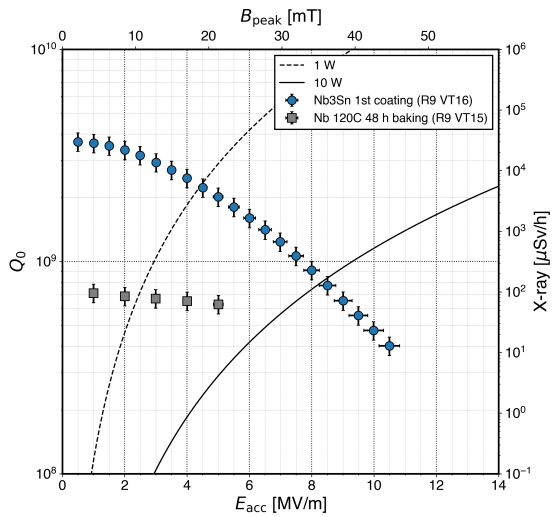

Figure 2: $Q - E$ curves measured at 4.2 K for the single-cell cavity before and after first coating.

SECOND AND THIRD Nb_3Sn COATING

After the RF measurement for the first-coated cavity, we found several points that need to be changed and began to modify them for the next coating on the cavity.

* hayato.ito@kek.jp

ISBN: 978-3-95450-234-9 ISSN: 2673-5504 doi:10.18429/JACoW-SRF2023-TUPTB014

Modifications

The Sn crucibles we had been using had an internal structure that was long and narrow as shown in Fig 3. Therefore, it was difficult to evaporate a sufficient amount of Sn. In the first coating, a large amount of Sn was put into the Sn crucible, and by keeping the Sn liquid level in the Sn crucible high during the coating step, the solid angle of the liquid level was widened and sufficient Sn was evaporated. However, this method left Sn in the Sn crucible after coating, which was expected to cause Sn contamination on the Nb_3Sn film, therefore, a new Sn crucible was fabricated that would allow Sn to be completely evaporated. The inner diameter of the new Sn crucible is ϕ 14 mm and its length is 15 mm. This gives an effective aperture of ϕ 26 mm, more than twice that of the conventional crucible, allowing all the Sn placed in the crucible to evaporate.

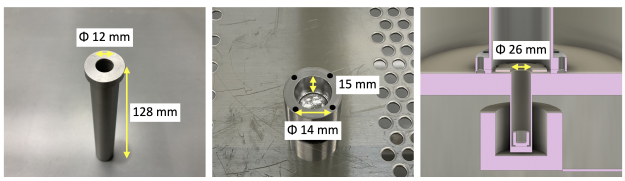

Figure 3: Sn crucible we used for first coating (left), new Sn crucible (center), cross-section of bottom of coating furnace with new Sn crucible (right).

Other modifications include a clean booth around the cavity installation port to prevent dust from entering the coating furnace during cavity installation as shown in Fig. 4. In addition, the top flange of the cavity was covered with Nb foil to prevent dust from entering the cavity. This is also to increase the Sn vapor pressure to ensure a more uniform distribution of the Sn vapor in the cavity.

Figure 4: Newly installed clean booth.

Cavity Coating

The above modifications have made it possible to evaporate the target amount of Sn without excess or deficiency and to perform the coating in a cleaner environment. For the second and third coatings, 2.0 g of Sn was put in the new Sn crucible and completely evaporated. However, this resulted in the formation of dots on the upper side of the inner surface of the cavity as shown in Fig. 5. In the second coating, there was a Sn droplet on the center of each dot. In the third coating, there were dots but no Sn droplets as seen in the second coating. After inspecting the inner surface, the third-coated cavity was reinstalled in the furnace and annealed at 1100 °C for 3 hours, but no visible change in the dots occurred. In both coatings, the dots were formed only on the upper side of the inner surface of the cell and not on the lower side.

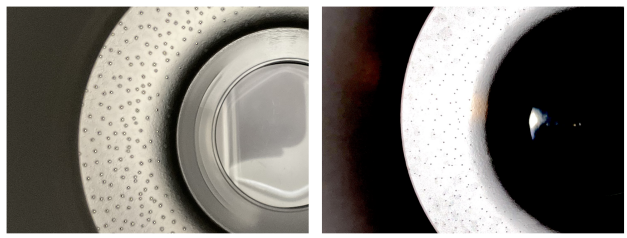

Figure 5: Upper side of the inner surface of the cavity cell in second coating (left) and third coating (right).

Free Molecular Flow Simulation on Sn Vapor

We used the COMSOL Multiphysics® software and the Molecular Flow Module to simulate the dilute flow of the Sn vapor at the beginning of the coating process and to estimate the distribution of the Sn vapor dispersed in the cavity and incident on the cavity wall [15]. When a large amount of Sn vapor is evaporated, the Sn vapor should be considered as a continuum flow because the mean free path of the Sn vapor is shortened, but at the beginning of the coating process, the Sn vapor pressure is low, therefore it can be treated as a free molecular flow. By simulating the Sn vapor distribution during the initial coating process, we found that the Sn vapor evaporated from the Sn crucible spreads out and goes directly to the upper side of the cell as shown in Fig. 6.

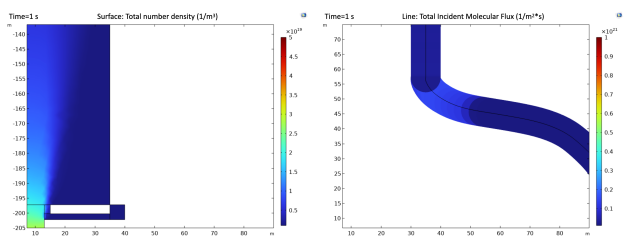

Figure 6: Total number density around the bottom flange (left) and total incident molecular flux to the upper side of the cell (right) in second and third coatings.

ISBN: 978-3-95450-234-9 ISSN: 2673-5504 doi:10.18429/JACoW-SRF2023-TUPTB014

Since the distribution of the incident Sn vapor simulated by COMSOL and the location of the dots in the cavity are in good agreement, it can simply be assumed that suppressing the incident to the upper side of the cell will result in suppressing the formation of the dots.

FOURTH Nb_3Sn COATING

The incident of the Sn vapor to the upper side of the cell can be suppressed by introducing an obstacle plate (shading) as shown in Fig. 7.

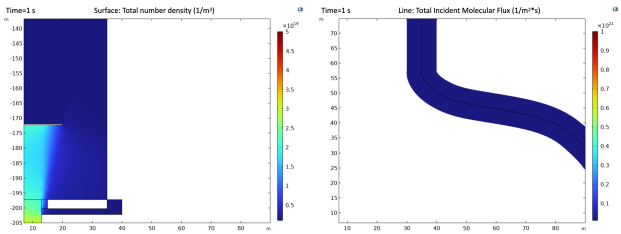

Figure 7: Total number density around the bottom flange (left) and total incident molecular flux to the upper side of the cell (right) in fourth coating.

Although a more complex shading or diffuser could be considered to suppress the incident of the Sn vapor while maintaining good Sn diffusion, we adopted this simplest idea for the fourth coating. The shading is made of Nb foil and the other parts are made of Mo. The diameter of the shading is ϕ 42 mm. The box made of Nb foil is for $SnCl_2$ (see Fig. 8).

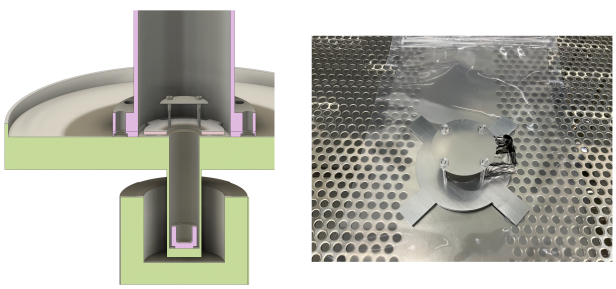

Figure 8: Cross-section of bottom of coating furnace and shading (left), and shading jig for fourth coating (right).

In addition, the cover of the top flange was newly fabricated with Mo as shown in Fig. 9. It was made wide enough (ϕ 200mm) to cover the flange sufficiently to prevent dust from entering the cavity during the cavity installation work and due to the impact of the vacuum pump. The gap between the Mo cover and the top flange was opened 10 mm to allow the excess Sn vapor in the cavity to escape during the coating step. In addition, from the second and third coating, it was found that the amount of Sn and $SnCl_2$ was excessive, therefore the Sn was reduced to 1.5 g and $SnCl_2$ was also reduced to 1.0 g for the fourth coating.

The parameters for each cavity coating are summarized in Table 1.

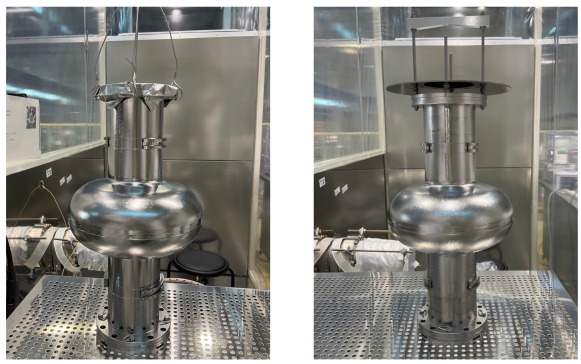

Figure 9: Setup of the cavity for third coating (left) and fourth coating (right).

Cavity Coating

Figure 10 shows the upper side of the inner surface of the cavity cell in the fourth coating and the SEM image of the witness sample. No dots were observed in the fourth-coated cavity. On the other hand, SEM analysis of the witness sample shows that the center of the Nb_3Sn grains appears dark and concave, indicating the lack of Sn in the Nb_3Sn grains. These results suggest that the three changes made for the fourth coating resulted in an insufficient supply of Sn vapor for Nb_3Sn formation.

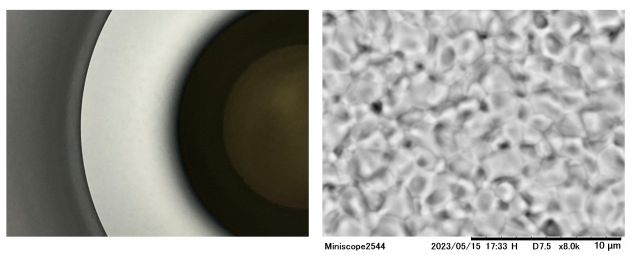

Figure 10: Upper side of the inner surface of the cavity cell in fourth coating (left) and SEM image of the witness sample (right).

RF MEASUREMENT

Figure 11 shows the $Q - E$ curves for all cavities coated with Nb_3Sn. The second-coated cavity in which the Sn droplets were observed could not be measured at 4.2 K due to its low Q_0. After cooling down to 2 K, the $Q - E$ curve could be measured and the Q_0 is 6.0×10^8. On the other hand, the third-coated cavity shows a Q_0 of 1.1×10^{10} at 4.2 K, although there were still dots on the inner surface. However, a significant Q-slope was observed from 6 MV/m, possibly due to additional annealing. The fourth-coated cavity shows a Q_0 of 8.5×10^9 at 4.2 K and has the significant Q-slope from 4 MV/m.

Figures 12 and 13 show the BCS resistance (R_{BCS}) and the residual resistance (R_{res}) for cavities coated with Nb_3Sn except for the second-coated cavity. The first-coated cavity has the highest R_{BCS} at low field and R_{res} is low but has a strong slope. The third-coated cavity has the lowest R_{BCS}

ISBN: 978-3-95450-234-9 ISSN: 2673-5504 doi:10.18429/JACoW-SRF2023-TUPTB014

Table 1: Coating Parameters

No.	Nucleation	Coating Furnace / Crucible	Annealing	Sn [g]	Sn [g]	Cavity Open / Close	Shading
1	500 °C 4.5 h	1100 °C 3 h / 1400 °C 3 h	-	2.0	2.7	Open	-
2	600 °C 1 h	1100 °C 3 h / 1300 °C 3 h	-	2.0	2.7	Close	-
3	600 °C 1 h	1100 °C 3 h / 1300 °C 3 h	1100 °C 3 h*	2.0	2.7	Close	-
4	600 °C 1 h	1100 °C 3 h / 1300 °C 3 h	-	1.5	1.0	Half-open (10mm gap)	ϕ 42 mm Nb foil disk

*The cavity was removed from the furnace once and then reinstalled for annealing.

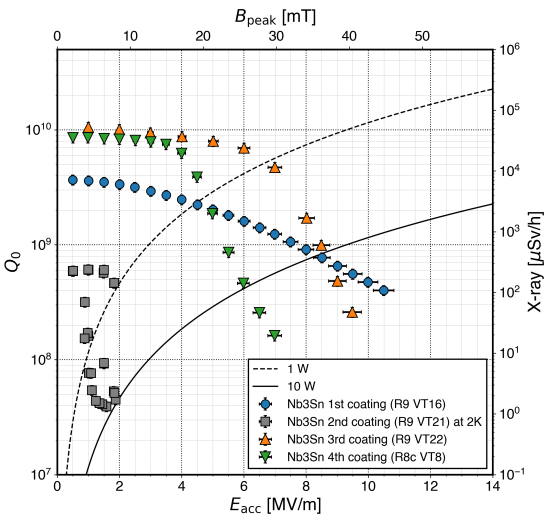

Figure 11: $Q - E$ curves for all cavities coated with Nb_3Sn.

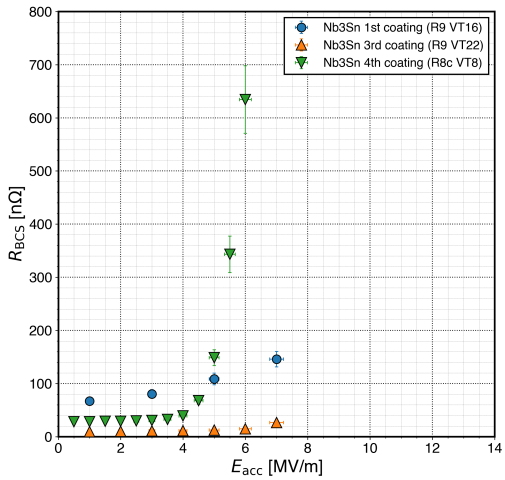

Figure 12: R_{BCS} for cavities coated with Nb_3Sn.

but the highest R_{res}. The fourth-coated cavity is in between for R_{BCS} but has the lowest R_{res}. However, both increase strongly from 4 MV/m. The third- and fourth-coated cavities behave similarly with respect to the $Q - E$ curve, but the R_{BCS} and R_{res} behaviors are opposite. This indicates that the characteristics of the Nb_3Sn film in the cavities might be essentially different between them. Nevertheless, what they have in common is the possible lack of Sn in the Nb_3Sn film. Resolving this would overcome the significant Q-slope.

CONCLUSION

We have performed four Nb_3Sn coatings on single-cell cavities with various modifications. Modification of the Sn crucible and installation of a clean booth has allowed Nb_3Sn coating in a more controlled Sn evaporation and cleaner environment. The cavity performance is steadily improving, although optimization of the coating parameters such as the amount of Sn source, Sn vapor control, and heat treatment steps is still in progress. We plan to continue to optimize parameters and start with improvements related to source amount and shading in the next coating.

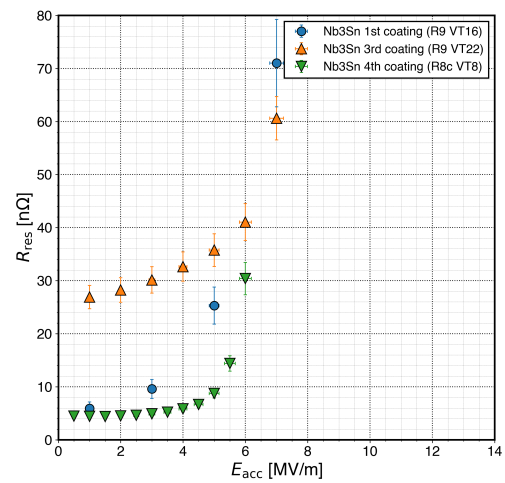

Figure 13: R_{res} for cavities coated with Nb_3Sn.

ACKNOWLEDGEMENTS

We would like to thank Taro Konomi for constructing the furnace and for his help in understanding the characteristics of the furnace. Also, We are grateful to Eiji Kako for his help in promoting our study.

ISBN: 978-3-95450-234-9 ISSN: 2673-5504 doi:10.18429/JACoW-SRF2023-TUPTB014

REFERENCES

[1] S. Posen and D. L. Hall, "Nb_3Sn superconducting radiofrequency cavities: fabrication, results, properties, and prospects", *Supercond. Sci. Technol.*, vol. 30, p. 033004, 2017. doi:10.1088/1361-6668/30/3/033004

[2] G. Ciovati *et al.*, "Development of a prototype superconducting radio-frequency cavity for conduction-cooled accelerators", *Phys. Rev. Accel. Beams*, vol. 26, no. 24, p. 044701, 2023. doi:10.1103/PhysRevAccelBeams.26.044701

[3] G. Ciovati *et al.*, "Multi-metallic conduction cooled superconducting radio-frequency cavity with high thermal stability", *Supercond. Sci. Technol.*, vol. 33, no. 7, p. 07LT01, 2020. doi:10.1088/1361-6668/ab8d98

[4] R. C. Dhuley *et al.*, "Development of a cryocooler conduction-cooled 650 MHz SRF cavity operating at ~10 MV/m cw accelerating gradient", *IOP Conf. Ser.: Mater. Sci. Eng.*, vol. 1240, no. 1, p. 012147, 2022. doi:10.1088/1757-899X/1240/1/012147

[5] R. C. Dhuley *et al.*, "First demonstration of a cryocooler conduction cooled superconducting radiofrequency cavity operating at practical cw accelerating gradients", *Supercond. Sci. Technol.*, vol. 33, no. 6, p. 06LT01, 2020. doi:10.1088/1361-6668/ab82f0

[6] N. Stilin *et al.*, "Stable CW Operation of Nb_3Sn SRF Cavity at 10 MV/m using Conduction Cooling", 2020. doi:10.48550/arXiv.2002.11755

[7] C. Dong *et al.*, "Preliminary Research of Niobium Cavity Coating with Nb_3Sn Film at IHEP", *Physica C*, vol. 600, p. 1354107, 2022. doi:10.1016/j.physc.2022.1354107

[8] S. Posen *et al.*, "Advances in Nb_3Sn superconducting radiofrequency cavities towards first practical accelerator applications", *Supercond. Sci. Technol.*, vol. 34, no. 2, p. 025007, 2021. doi:10.1088/1361-6668/abc7f7

[9] G. Eremeev *et al.*, "Nb_3Sn multicell cavity coating system at Jefferson Lab", *Rev. Sci. Instrum.*, vol. 91, no. 7, p. 073911, 2020. doi:10.1063/1.5144490

[10] U. Pudasaini *et al.*, "Analysis of RF losses and material characterization of samples removed from a Nb_3Sn-coated superconducting RF cavity", *Supercond. Sci. Technol.*, vol. 33, no. 4, p. 045012, 2020. doi:10.1088/1361-6668/ab75a8

[11] Z. Q. Yang *et al.*, "Development of Nb_3Sn Cavity Coating at IMP", in *Proc. SRF'19*, Dresden, Germany, Jun.-Jul. 2019, pp. 21–24. doi:10.18429/JACoW-SRF2019-MOP003

[12] R. D. Porter *et al.*, "Next Generation Nb_3Sn SRF Cavities for Linear Accelerators", in *Proc. LINAC'18*, Beijing, China, Sep. 2018, pp. 462–465. doi:10.18429/JACoW-LINAC2018-TUPO055

[13] K. Takahashi *et al.*, "Design and Construction of Nb_3Sn Vapor Diffusion Coating System at KEK", in *Proc. SRF'21*, East Lansing, MI, USA, Jun.-Jul. 2021, pp. 23-26. doi:10.18429/JACoW-SRF2021-SUPCAV008

[14] K. Takahashi *et al.*, "First Nb_3Sn Coating and Cavity Performance Result at KEK", in *Proc. SRF'21*, East Lansing, MI, USA, Jun.-Jul. 2021, pp. 27-31. doi:10.18429/JACoW-SRF2021-SUPCAV009

[15] COMSOL Multiphysics® v. 6.1. http://www.comsol.com